



FLOURY AND SHRUNKEN ENDOSPERM6 Encodes a Glycosyltransferase and is Essential for the Development of Rice Endosperm

Hang Yang¹ · Linglong Liu¹ · Kai Wu¹ · Shijia Liu¹ · Xi Liu¹ · Yunlu Tian¹ · Yunlong Wang¹ · Erchao Duan¹ · Jie Lei¹ · Xiuhao Bao¹ · Rongbo Chen¹ · Xiaoli Chen¹ · Yi Ji¹ · Yu Zhang¹ · Yihua Wang¹ · Jianmin Wan^{1,2}

Received: 25 July 2020 / Revised: 1 December 2020 / Accepted: 3 December 2020 / Published online: 20 January 2021
© Korean Society of Plant Biologist 2021

Abstract

Composition and structure of endosperm starch are major determinant factors for rice quality. Glycosylinositol phosphorylceramides (GIPC) is a kind of sphingolipid and it accounts for ~25% of total plasma membrane lipids in plants. The relationship between synthesis of GIPC and development of endosperm starch, however, remains unclear. We here identified a mutant with a floury and opaque endosperm, named *floury and shrunken endosperm 6* (*fse6*). The mutant seeds displayed a shrunken grain appearance. Physicochemical analysis showed that both total starch and amylose contents were decreased, while lipid and protein contents were increased in the mature mutant seeds, compared to their counterparts in the wild type. Further observation of semi-thin sections indicated the development of mutant amyloplasts was defective. The mutant seeds germinated normally but failed to survive in a later stage of seedling growth. Map-based cloning and genetic complementation revealed that *FSE6* encodes a glycosyltransferase and is homologous to Arabidopsis GLUCOSAMINE INOSITOLPHOSPHORYLCERAMIDE TRANSFERASE1 (GINT1), an enzyme vital for GIPC synthesis. We further found that cellulose content and starch biosynthesis in the mutant were altered. This study connects a gap between a rice GINT1 and starch synthesis, which will be helpful for rice quality improvement.

Keywords Floury endosperm · Glycosylinositol phosphorylceramides (GIPCs) · Glycosyltransferase (GT) · Cellulose synthesis · Starch biosynthesis

Hang Yang and Linglong Liu contributed equally to this work.

Supplementary Information The online version contains supplementary material available at <https://doi.org/10.1007/s12374-020-09293-z>.

✉ Yihua Wang
yihuawang@njau.edu.cn

✉ Jianmin Wan
wanjm@njau.edu.cn; wanjianmin@caas.cn

¹ State Key Laboratory for Crop Genetics and Germplasm Enhancement, Jiangsu Plant Gene Engineering Research Center, Nanjing Agricultural University, Nanjing 210095, People's Republic of China

² National Key Facility for Crop Resources and Genetic Improvement, Institute of Crop Science, Chinese Academy of Agricultural Sciences, Beijing 100081, People's Republic of China

Introduction

With the increasing production of rice (*Oryza sativa*), the public has higher and more diverse requirements for its quality. The rice endosperm accumulates a lot of starch during the maturation process, which exists in the amyloplast and is the main carbon source for humans and livestock (Burrell 2003; Seung and Smith 2019). Insufficient starch filling will lead to an opaque floury phenotype of endosperm due to the large number of voids inside. Therefore, screening floury endosperm mutants can help us study the mechanism of starch synthesis, so as to improve rice quality.

To date, a series of genes that affect endosperm starch synthesis have been identified in rice (Kang et al. 2005; Zhang et al. 2016; Zhu et al. 2018; Hao et al. 2019; Wu et al. 2019; You et al. 2019). *FLO4* (*FLOURY ENDOSPERM4*) encodes pyruvate orthophosphate dikinase (PPDK), which catalyzes the conversion of pyruvate to phosphoenolpyruvate, regulating carbon metabolism and starch synthesis during grain filling (Kang et al. 2005); *FLO6* encodes a protein

that contains a CBM48 domain, and its mutation results in lower starch content and different sizes of rice amyloplasts. Likewise, *Arabidopsis FLO6* is involved in the initiation of starch synthesis (Peng et al. 2014). Mutations in two pentatricopeptide repeat (PPR) proteins FLO10 and OsNPPR1, which are located in the mitochondria and nucleus, respectively, also cause defects in endosperm starch synthesis (Hao et al. 2019; Wu et al. 2019). These studies reveal that starch synthesis involves a variety of physiological and biochemical processes, including substance metabolism and signal regulation.

Glycosylinositol phosphatidylceramides (GIPC) are the major sphingolipids in the plant plasma membrane. It was estimated GIPC make up about a quarter of plasma membrane lipid in the *Arabidopsis* leaves (Markham and Jaworski 2007; Jean-Luc et al. 2016; Ishikawa et al. 2018). Recently, many studies revealed that GIPC, apart from as membrane component and organization (Mongrand et al. 2004; Jean-Luc et al. 2016), participates also in various physiological activities like pollen development (Rennie et al. 2014), symbiosis (Perotto et al. 1995), defense against pathogens (Mortimer et al. 2013; Tartaglio et al. 2016). Enzymes involved in GIPC biosynthesis have been widely studied in *Saccharomyces cerevisiae* (Markham and Jaworski 2007). The ceramide backbone is synthesized in the endoplasmic reticulum (ER). First, serine and palmitoyl-CoA are catalyzed by serine palmitoyltransferase to produce 3-ketopurine, which is then reduced to long-chain base (LCB) dihydrosphingosine (d18:0) by 3-ketopurine reductase. Dihydrosphingosine eventually forms ceramide through hydroxylation or desaturation (Chen et al. 2007). Mature GIPCs are synthesized in the Golgi apparatus. IPC synthase adds inositol phosphate groups to ceramide to form inositol phosphorylceramide (IPC) (Figure S1), which were then modified by various glycosyltransferases (GTs) (Wang et al. 2008). IPC biosynthesis is highly conserved between plants and fungi (Dunn et al. 2004) but the glycan patterns vary among plant species and tissues. INOSITOL PHOSPHORYLCERAMIDE GLUCURONOXYLTRANSFERASE1 (IPUT1) is the first identified glycosyltransferase in *Arabidopsis thaliana* which can convert Glucuronic acid (GlcA) from UDP-GlcA to IPC and eventually form GlcA-IPC (Rennie et al. 2014). In *Arabidopsis* vegetative tissues, a transporter GOLGI-LOCALIZED NUCLEOTIDE SUGAR TRANSPORTER1 (GONST1) is responsible for transferring GDP-Man into the Golgi, and then transferring mannose (Man) to GlcA-IPC via GIPC MANNOSYL-TRANSFERASE1 (GMT1) to complete the further glycation modification process (Mortimer et al. 2013; Fang et al. 2016). However, in *Arabidopsis* seeds and pollen as well as in rice and tobacco plants another glycosyltransferase, viz. GLUCOSAMINE INOSITOLPHOSPHORYLCERAMIDE TRANSFERASE1 (GINT1), is responsible for transferring GlcN(Ac) to GIPC (Fang et al. 2016). The loss

of key genes associated with GIPCs synthesis demonstrates a variety of effects on plant growth and development, including impaired pollen tube germination, dwarfing of plants, lethality at seedling stage, and defensive responses (Baldwin et al. 2001; Singh et al. 2005; Rennie et al. 2014; Fang et al. 2016; Ishikawa et al. 2018). However, there is no report on the relationship between GIPC glycosylation and rice endosperm development.

In our study, we obtained a mutant named *floury and shrunken endosperm 6 (fse6)* with opaque and floury brown rice, whose homozygous seeds can germinate normally but cannot survive at a later seedling stage. Through map-based cloning and genetic complementation, we determined that these defects were caused by the mutation of a glycosyltransferase 64 (GT64). Previously, gene knockout of the GT64 in rice leads to a phenotype of lethal seedling and decreased GIPC glycosylation (Ishikawa et al. 2018). Analysis of semi-thin sections showed that starch grains (SGs) of the mutant seeds were unshaped and loose, and gene expression involved in starch metabolism was changed, compared with the wild type. This indicates that the misglycosylation of GIPC affects the starch biosynthesis in rice endosperm. Moreover, we found that cellulose content of *fse6* is significantly decreased relative to the wild type, indicating that the integrity of the plasma membrane lipid structure may be necessary for cellulose synthesis.

Results

The *fse6* Mutant has Floury Endosperm and is Lethal at Seedling Stage

To improve rice quality by mutagenesis, we treated a *japonica* elite variety Ningeng4 (NG4) with Methyl nitrosourea (MNU) at the flowering stage, and selected a floury endosperm mutant *fse6*. The mutant showed a defective grain development with opaque and shrunken seeds at maturity, in contrast to transparent grain of the wild type (Fig. 1a, b). Observation of seed cross-section indicated that core endosperm of the mutant displayed a floury-white phenotype, whereas peripheral endosperm and aleurone layer were normal and similar to the wild type (Fig. 1c, d). There is no significant difference of grain length and width between the mutant and its wild type, but grain thickness and 1000-grain weight were obviously decreased in the mutant relative to the wild type ($p < 0.01$, Fig. 1i, j). The mutant seeds were capable to germinate normally, but the resultant seedlings failed to survive after two-leaf stage (Fig. 1k). Scanning electron microscopic (SEM) showed that, instead of the tightly packed and polygonal starch granules of wild type, the mutant displayed loosely packed and non-shaped starch granules (Fig. 1e–h).

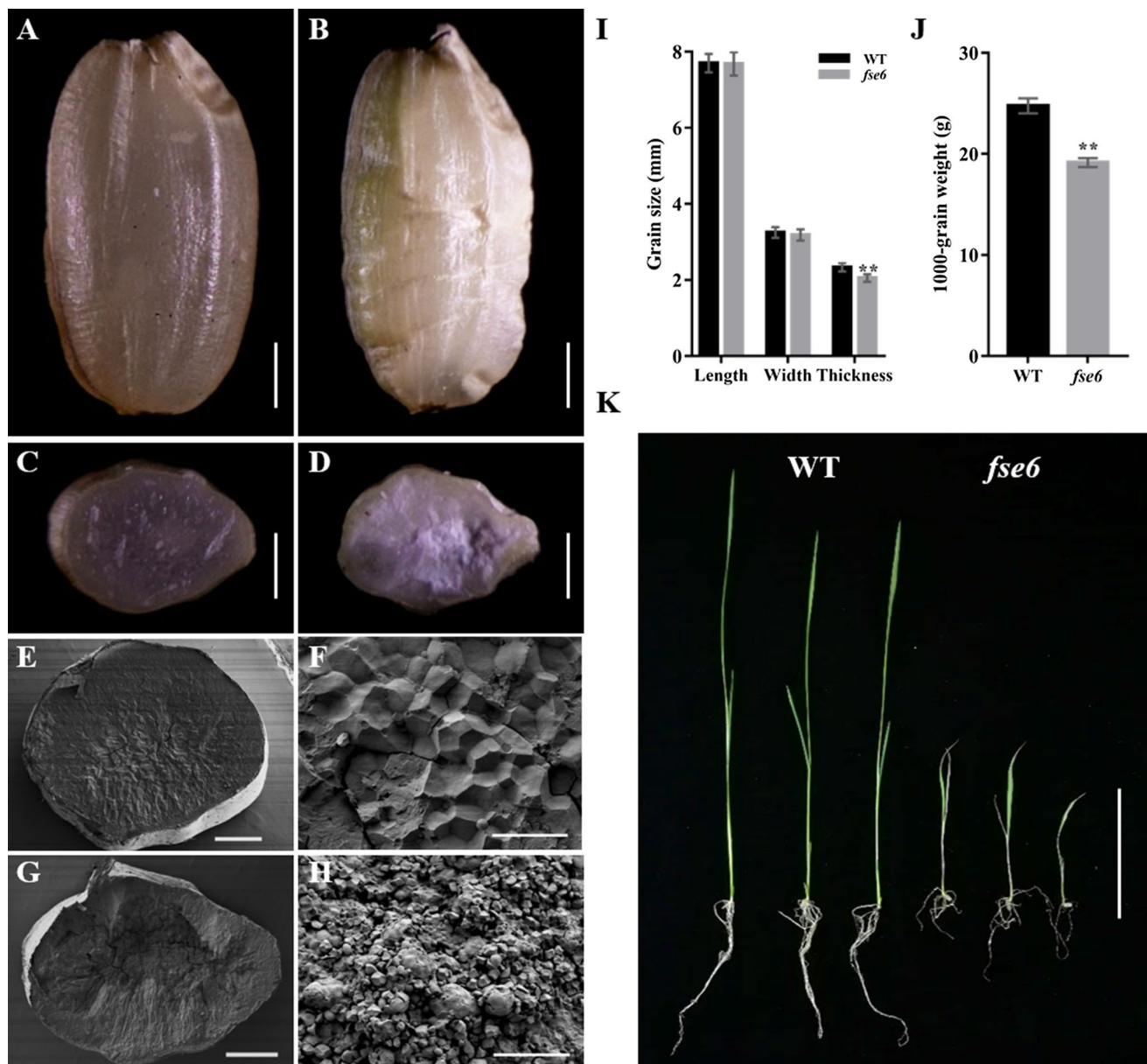


Fig. 1 The *fse6* mutant has floury endosperm and is lethal at seedling stage. **a, b** Comparison of wild-type NG4 and *fse6* mutant mature seeds, bars: 1 mm; **c, d** cross-sections of wild-type and *fse6* mutant seeds, bars: 1 mm; scanning electron microscopy images of transverse sections of wild-type (**e, g**) and *fse6* mutant (**f, h**) seeds. Bars: 1 mm in (**e, g**). Bars: 30 μ m in (**f, h**); **i** Comparison of grain size

between the wild type and *fse6* mutant, values are means \pm standard derivation (SD), $n=20$ for each sample; **j** Comparison of 1000-grain weight of the wild type and *fse6* mutant, $n=3$; **k** Young seedlings of wild-type and *fse6* mutant at 14 days after germination, bar: 3 cm. The significance of the data was analyzed by Student's *t* test in (**i, j**), ** $p < 0.01$

Analysis of Physical and Chemical Properties of Mature Seeds

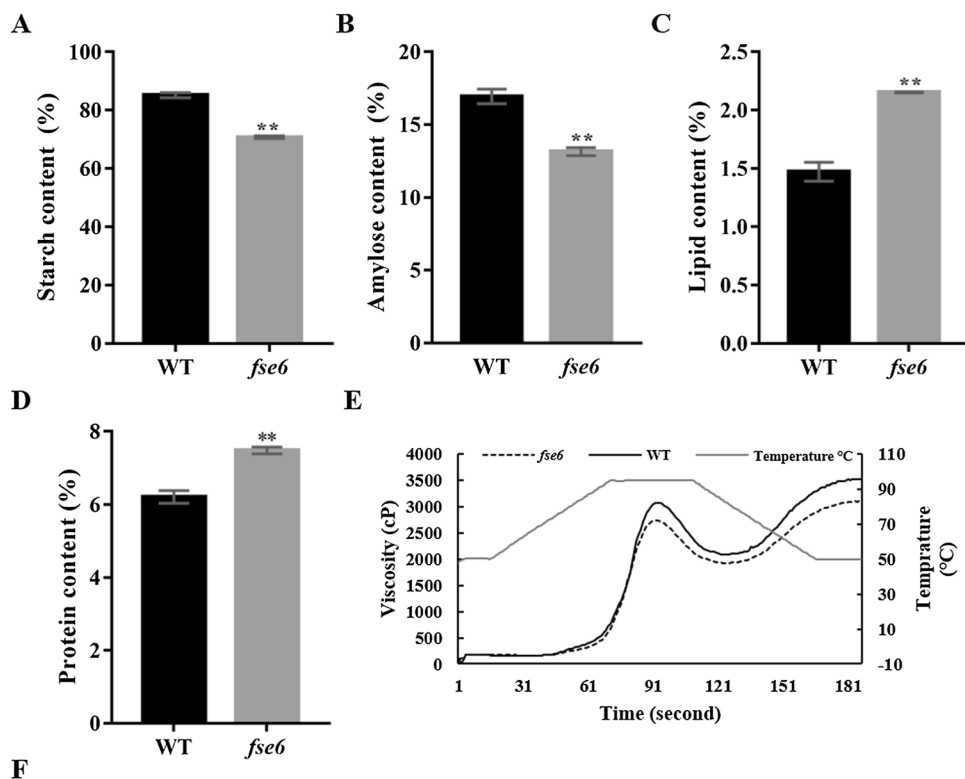
Total starch and amylose contents of the mutant were both significantly lower than those of the wild type (Fig. 2a, b), but lipid and protein contents were significantly higher than wild type (Fig. 2c, d). Viscosity analysis indicated that the starch setback value (SBV), consistence value (CSV) and breakdown value (BDV) were slightly decreased in the

mutant (Fig. 2e, f). Overall, the physical and chemical properties of the *fse6* mature seeds vary greatly compared to the wild type.

Development of Starch Grains in *fse6* Mutants is Abnormal

To further investigate whether the starch biosynthesis of the mutant is defective, we observed the developing endosperm

Fig. 2 Analysis of physical and chemical properties of mature seeds. Determination of total starch (a), amylose (b), lipid (c), and protein (d) contents in the wild-type and *fse6* mutant seeds. Values are means \pm SD, $n=3$. The significance of the data was analyzed by Student's *t* test, $**p < 0.01$. e–f Rapid visco analysis (RVA) profiles of the wild-type and mutant endosperm starch. *F* indicates the values of some specific points in *E*



| Test | Peak Viscosity | Hot paste viscosity | Breakdown Value | Cool paste viscosity | Setback Value | Peak time | Pasting Temp |
|-------------|----------------|---------------------|-----------------|----------------------|---------------|-----------|--------------|
| WT | 3074 | 2092 | 982 | 3527 | 453 | 6.2667 | 89.35 |
| <i>fse6</i> | 2742 | 1921 | 821 | 3108 | 366 | 6.2 | 89.35 |

at 9 days after flowering (DAF). Semi-thin section indicated a lot of intact, regular and armor-like polygonal compound SGs were observed in the wild type (Fig. 3a, d). In comparison, the mutants showed large amounts of broken and unformed single starch granules. There were many cavities in the mutant endosperm, which may be the reason for the opaque appearance (Fig. 3b, c, e, f). Moreover, we found that the amyloplast development of the mutant was significantly delayed than that of the wild type.

Map-Based Cloning and Complementation Test

To find the gene responsible for the floury-white endosperm of the mutant, the mutant was crossed with *indica* cultivar Dular to construct an F_2 population. Initially *OsFSE6* was located in an interval of 5.4 cM on the chromosome 5 with 10 recessive individuals selected from the F_2 segregating population (Fig. 4a). Next, the mapping interval was narrowed into 240 kb between SSR markers F2-1 and F2-5 with other 415 opaque individuals. In this region, there exist 30 candidate genes predicated by the Rice Expression Profile Database (<http://ricexpro.dna.affrc.go.jp/>). By sequencing, a single nucleotide change from cytosine (C) to adenine (A)

were found in the *Os05g0540000*, generating a premature stop codon in the mutant (Fig. 4b). By aligning the amino acid sequence at National Center for Biotechnology Information (NCBI, <https://www.ncbi.nlm.nih.gov/>), the candidate protein contains a glycosyltransferase domain (Fig. 4c), which was designated as OsGINT1 previously (Ishikawa et al. 2018).

To confirm the mapping result, we performed complementation test by transforming *pFSE6::OsFSE6* into the mutant callus. Positive transgenic lines were identified by PCR and they could survive over the whole seedling stage and produce transparent and normal seeds (Fig. 4d, e). Thus, the *Os05g0540000* corresponds to the *FSE6* gene.

Subcellular Localization and Phylogenetic Analysis of OsFSE6

To explore biochemical function of the OsFSE6, we fused its full-length cDNA with green fluorescent protein (GFP) and observed their transient expression on *N. tabacum* leaf epidermal cells. As shown in confocal laser scanning microscopy, green fluorescent signals were completely overlapped with the Golgi marker α -mannosidase 1 (GmMan1)

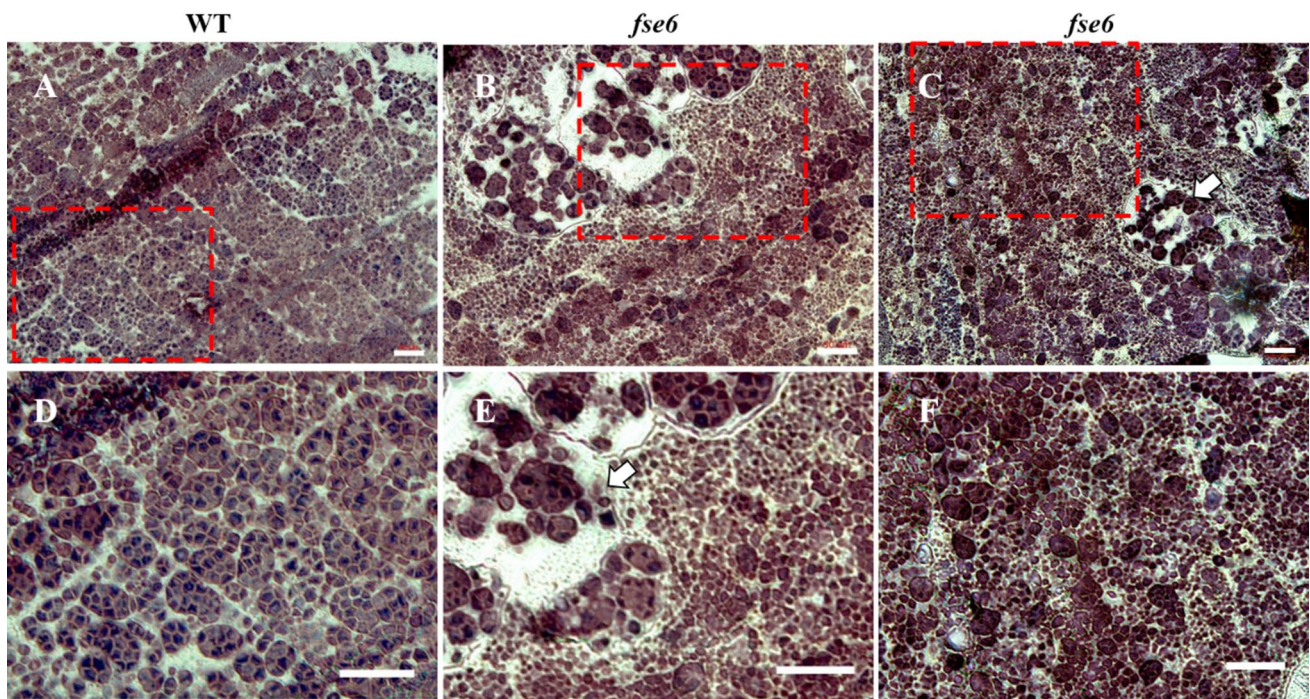


Fig. 3 Development of starch grains in the *fse6* mutant is abnormal. Semi-thin sections of wild-type (a, d) and *fse6* (b, c, e, f) endosperm at 9 days after flowering (DAF). d, e and f is the enlargement of the

area in the red frame corresponding to a, b and c. Bars: 50 μm in (a–f). The white arrow indicates the cavity formed due to insufficient starch filling

(Rennie et al. 2014), but not with prevacuolar compartments (PVCs) marker vacuolar sorting receptor 2 (VSR2) (Miao et al. 2006) (Fig. 5a).

Next, we constructed a phylogenetic tree to explore the homology of this glycosyltransferase among different species. The *OsFSE6* protein shared high sequence similarity (> 80%) with its homologs in *Zea mays* and *Sorghum bicolor*, and 50% with Arabidopsis FSE6 (Fig. 5b). BLAST search of the NCBI database also identified two paralogs of *OsFSE6* in rice genome, with amino acid sequence similarity of 52.6 and 11.7%, respectively. Sequence alignment revealed that, despite of relative low similarity, *OsFSE6* and its two paralogs all harbored a highly conserved glycosyltransferase domain, and this domain was also conserved in plants (Fig. S2, S3). According to a previous grouping method (<http://cys.bios.niu.edu/plantcazyme/>) (Ekstrom et al. 2014), *OsFSE6* belongs to a member of GT64 subfamily.

Expression Pattern of FSE6 and its Homologs

qRT-PCR analysis showed that the *OsFSE6* was constitutively expressed in various tissues, including roots, stems, leaves, sheaths, and panicles. *OsFSE6* was also pronounced during endosperm development (Fig. 6a). Compared with the other two *OsFSE6* homologs, the expression of *OsFSE6* was obviously higher in all tested tissues (Fig. 6b). The

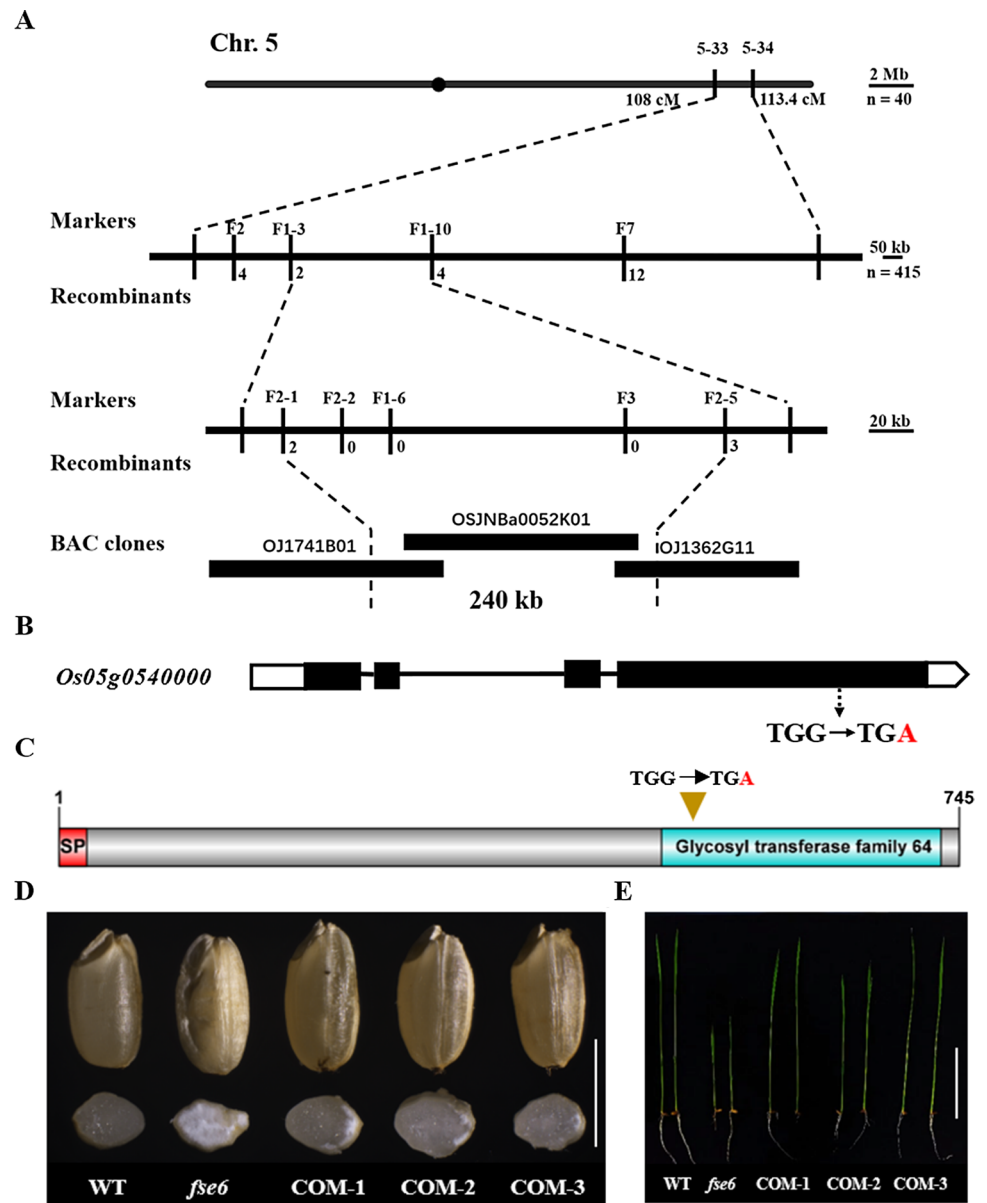
qRT-PCR experiments were consistent with histochemical staining assay of transgenic plants expressing the GUS reporter gene driven by the native *OsFSE6* promoter (Fig. 6c–g).

Starch Biosynthesis and Cellulose Synthesis are affected in the *fse6* Mutants

Semi-thin section indicated that the mutant had defective amyloplast development, thus we further tested expression level of genes involved in starch synthesis. Quantitative results showed that starch synthase IIb (SSIIb), granule-bound starch synthase II (GBSSII) and disproportionating enzyme IIa (DPEIIa) were significantly down-regulated, while the expression of starch synthase I (SSI), isoamylase (ISA) and starch branching enzyme IIb (BEIIb) has increased more than four times (Fig. 7a). Subsequent immunoblot analysis showed that the abundance of FLO4 protein was decreased in the mutant (Fig. 7b). FLO4 has previously been shown to regulate carbon metabolism and starch synthesis during endosperm filling (Kang et al. 2005). This indicates that the *fse6* endosperm starch synthesis is affected to some extent due to the *OsFSE6* mutation.

Previous studies revealed the degree of glycosylation of sphingolipids influences cellulose synthesis via glycosyltransferase (Fang et al. 2016). Moreover, deficiency of sphingolipid triggers a constitute hypersensitive response in

Fig. 4 Map-based cloning and complementation test of *FSE6*. **a** Fine mapping of the *FSE6* locus. The *FSE6* locus was mapped to a 241-kb region between markers F2-1 and F2-5 on chromosome 5 (Chr.5). The molecular markers and the number of recombinants is indicated on the map. cM, centimorgan. **b** Schematic diagram of *FSE6* gene structure and mutation site. The white boxes represent untranslated regions, the black boxes represent exons, and the lines represent introns. Single-base mutation from G to A (in red) causes premature termination of the translation. **c** Schematic diagram of the *FSE6* protein structure, which is predicted to carry a signal peptide (SP) at the N-terminus and a glycosyltransferase domain between the 499th and the 730th amino acids. Arrow indicates the mutation site. **d** Seed appearance and cross-sections of seeds from the wild type, *fse6* mutant, and transgenic complementary lines. Bar: 8 mm. **e** Seedling appearance of the wildtype, *fse6* mutant, and transgenic complementary lines, bar: 3 cm. COM-1, COM-2, COM-3 represent three independent transgenic lines (**d**, **e**)



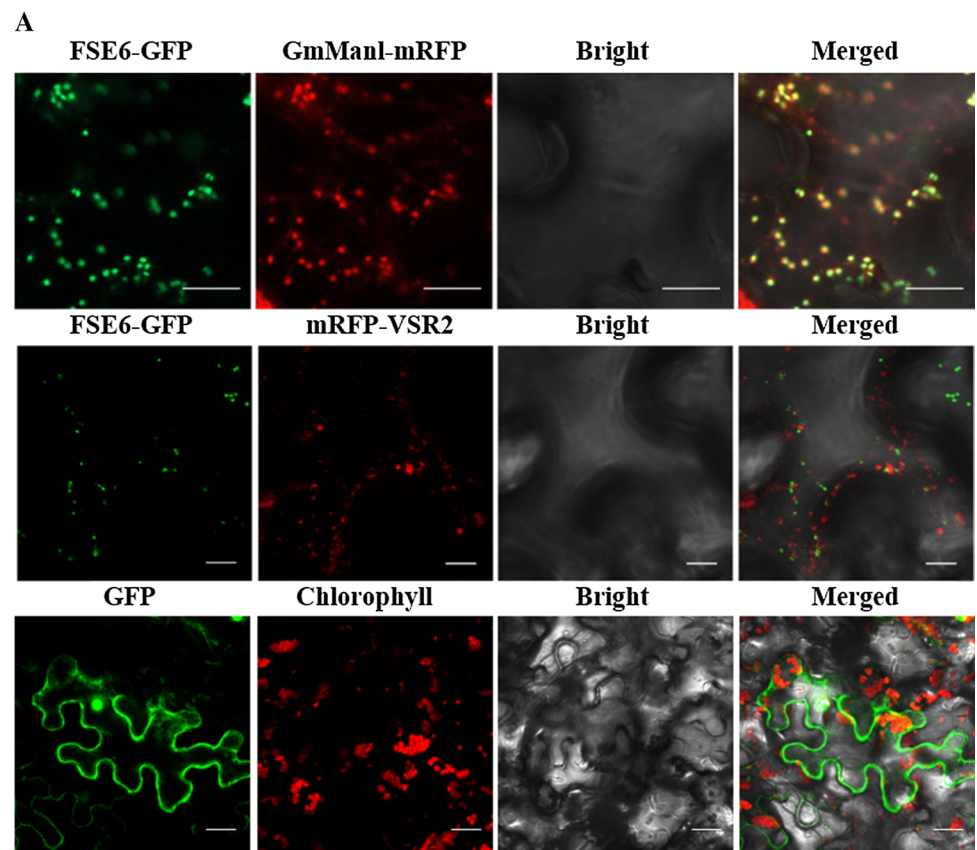
Arabidopsis characterized by increased levels of hydrogen peroxide and salicylic acid (Rennie et al. 2014; Fang et al. 2016). Hence, we measured the cellulose and H₂O₂ contents in the *fse6* seedlings. Compared with the wild type, the mutant exhibited a slight but significant decrease in cellulose content (Fig. 7c). There was no statistic difference in the content of H₂O₂ between the mutant and its wild type (Fig. 7d).

Discussion

In this study, we isolated and characterized the *fse6* mutant whose brown grain was floury and shrunken. Scanning electron microscopy (SEM) showed that, instead of the

tightly packed and polygonal starch granules of wild type, the mutant displayed loosely packed and non-shaped starch granules (Fig. 1e–h). Compared with the wild type, the *fse6* mutant exhibited lower starch and amylose contents and higher protein and lipid contents (Fig. 2a–d). Semi-thin sections of 9 DAF endosperm indicated a lot of intact, regular and armor-like polygonal compound starch grains (SGs) were observed in the wild type (Fig. 3a, d). In comparison, the mutants showed large amounts of broken and unformed single SGs (Fig. 3b, c, e, f). Through map-based cloning and genetic complementation (Fig. 4a–e), we showed that the disfunction of a glycosyltransferase is responsible for these phenotypes. In addition, the expression of starch synthesis-related genes in the *fse6* mutants was affected (Fig. 7a). This reveals that sphingolipid

Fig. 5 Subcellular localization and phylogenetic analysis of FSE6. **a** Subcellular localization of OsFSE6 protein in tobacco epidermal cells. OsFSE6 protein subcellular localization in tobacco epidermal cells. GmMan1 and VSR2 are two control proteins that localize to the Golgi and prevacuolar compartments (PVCs), respectively. Bars: 5 μm in the second row, 10 μm in the top row and the last row. **b** Phylogenetic tree of *OsFSE6* (in red) and its homologs constructed using MEGA 5



biosynthesis is involved in starch biosynthesis, thereby affecting rice endosperm development and grain quality. As glycosylated sphingolipids participate in a wide range of biochemical activities (Perotto et al. 1995; Mongrand et al. 2004; Mortimer et al. 2013), but there is still no

report that they affect starch synthesis. The lethality of the mutant at the seedling stage indicates that many processes of its life cycle are severely damaged. We speculate that starch biosynthesis defect may be a secondary effect of GIPC's mis-glycosylation.

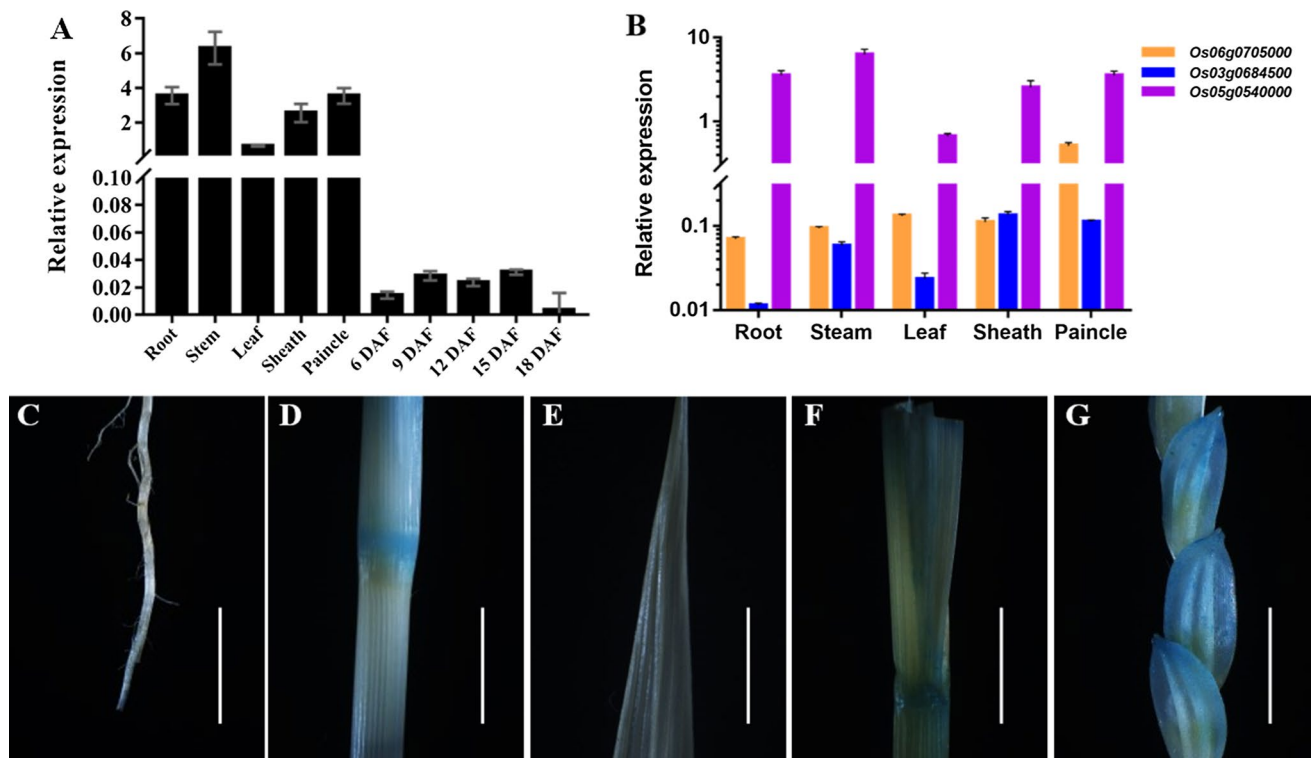


Fig. 6 Expression pattern of *FSE6* and its homologs. **a** Expression levels of *OsFSE6* in the various tissues and different developmental stages of endosperm in the wild type and *fse6* mutant. *Actin1* was used as an internal control. Values are means \pm SD ($n=3$). DAF,

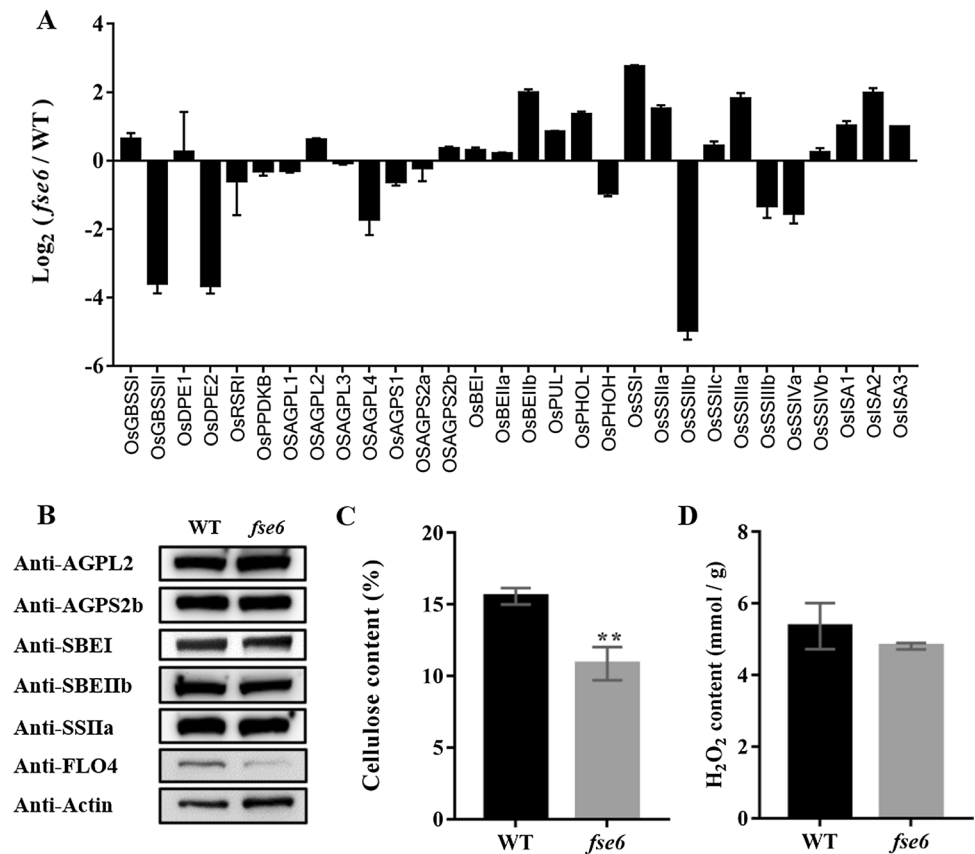
days after flowering. **b** Expression levels of *OsFSE6* and its paralogs in different tissues. GUS staining of various tissues in the *pOsFSE6::GUS* transgenic lines, including root (c), stem (d), leaf (e), sheath (f), and panicle (g). Bars: 1 cm

Previously it was reported that a homologous gene of the *OsFSE6* in Arabidopsis, named *AtGINT1*, is responsible for transferring *N*-acetylglucose (GlcNAc) to GIPC (Ishikawa et al. 2018). When the *OsGINT1* (*Os05g0540000*) was knocked out in rice, the plants could only survive for about 2 weeks on the growth medium and the glycosylation of sphingolipid in seedlings was also decreased significantly (Ishikawa et al. 2018). Consistent with the previous results, the *fse6* mutant seeds germinated normally, but the seedlings died after two-leaf stage (Fig. 1k). Besides, the loss of GlcNAc to GIPC synthesis in *atgint1* mutant was completely recovered by expressing *OsGINT1* under *AtGINT1*'s promoter (Ishikawa et al. 2018). Together with our study, it indicated *OsFSE6* could partially substitute the role of *AtGINT1* for plant GIPC synthesis.

Nevertheless, the *atgint1* mutants grow normally on agar and soil under standard conditions, and shows no gross morphological phenotype compared to that of its wild type. Meanwhile, the seed coat of *atgint1* is normal, and has a normal distribution of oil and starch bodies (Ishikawa et al. 2018). Unlike Arabidopsis *atgint1* mutant, the development of rice *fse6* plants and seeds is severely hindered, and the entire surface of homozygous *fse6* grain is shrunk. TEM and semi-thin sections revealed that the *fse6* amyloplasts were

disrupted. One reason for the lethality at the seedling stage can be that *OsFSE6* is constitutively expressed in all tissues such as roots, stems, leaves, sheaths, and panicles (Fig. 6a, c–g). The absence of *OsGINT1* is expected to have a comprehensive impact on the overall development of plants. In comparison, Arabidopsis *AtGINT1* is only highly expressed in reproductive tissues such as developing embryos and mature seeds, as well as in pollen and stigma. In Arabidopsis vegetative organs, a paralog of *AtGINT1*, *AtGMT1*, is responsible to transfer Mannose to GIPC (Ishikawa et al. 2018), and the *gmt1* mutant plant has a dwarfed phenotype, and can only produce a few viable seeds (Fang et al. 2016). *OsFSE6* also has two paralogs (Fig. 5b), but their expression levels are much lower in all tissues (Fig. 6b). This suggests that *OsFSE6* may play a major role in rice plant and endosperm development. In addition, the *atgmt1* mutant displays constitutive salicylic acid and hydrogen peroxide accumulation (Fang et al. 2016). We here observed that cellulose content of *fse6* was also significantly decrease (Fig. 7c). In contrast, *fse6* showed no significant difference in H_2O_2 level compared to its wild type (Fig. 7d). GIPC is modified with sugar groups in the Golgi apparatus and then transported to the plasma membrane (Fang et al. 2016). CTL1 and COBRA, two extracellular proteins anchored to the plasma membrane

Fig. 7 Starch biosynthesis and cellulose synthesis are affected in the *fse6* mutant. **a** Expression of the genes related to starch synthesis in endosperm of wild type and mutant at 12 days after flowering. *Actin1* was used as an internal control. Values are means \pm SD, $n = 3$. **b** Immunoblot analysis of starch biosynthesis related proteins in mature seeds of wild type and *fse6* mutant. *Actin1* was used as a reference protein. **c** Determination of cellulose content in the wild-type and mutant seedlings. Values are means \pm SD, $n = 3$. **d** Determination of hydrogen peroxide content in wild-type and mutant seedlings. Values are means \pm SD, $n = 3$



via glycosylphosphatidylinositol, can affect the mobility of the cellulose synthase (CESA) complex (McFarlane et al. 2014). Similarly, the mis-glycosylation of GIPC may affect the movement of the CESA synthase complex or associated proteins, resulting in impaired cellulose synthesis in the mutant.

We here identified the *OsFSE6*, different from its counterpart in Arabidopsis, is essential for both rice plant and endosperm development. Regulation of sphingolipid synthesis through *OsFSE6* will open a new window for improving rice endosperm quality.

Methods

Plant Materials and Growth Conditions

The *fse6* mutant with defects in grain development was selected by large-scale screening of a *japonica* variety Ninggeng4 (NG4) mutant bank treated with Methyl nitrosourea (MNU). All plants were grown in natural and well-managed fields or plant growth chambers (12 h of light/12 h of darkness at 30 °C) at Nanjing Agricultural University, Jiangsu, China (32° 2', 118° 50'). Endosperm at 6–21 days after flowering (DAF) and mature seeds were collected immediately and used for further experiments or stored in

– 80 °C ultra-low temperature refrigerator (F570, Eppendorf). Homozygous *fse6* mutant was collected and kept from heterozygous *fse6* plants.

Microscopy

The mature seeds for scanning electron microscopy were prepared as described previously (Peng et al. 2014) and observed with a HITACHI S–3400 N scanning electron microscope. For amyloplast observation, seeds of a certain developing period were cut into 1–2 mm thick and fixed in 0.1 M phosphate buffer (pH 7.2) with 2% (v/v) glutaraldehyde and 2% (w/v) paraformaldehyde overnight. Then the sample was embedded in resin as described previously (Takemoto et al. 2002). Finally, 1 μm sections were prepared, and then stained with I₂-KI (0.5%) and observed under a microscope (80i, Nikon).

Determination of Seed Physiological and Biochemical Indexes

Starch content of brown rice flour was measured with a starch assay kit, following the manufacturer's instruction (Megazyme, Wicklow). Amylose, protein and lipid content were determined following the method mentioned previously (Liu et al. 2009). The pasting properties of endosperm starch

were tested with a same method as described before (Peng et al. 2014).

Map-Based Cloning and Complementation Analysis

The *fse6* heterozygous plant was crossed with an *indica* variety Dular to produce hybrids, and the hybrids was self-pollinated to generate an F₂ population. Recessive individuals with *fse6* like phenotype in the F₂ population were selected for gene rough mapping. For fine mapping, total 14 SSR (simple sequence repeat) markers were developed based on the sequence polymorphism of the two parents (Table S1).

Full-length cDNA of *FSE6* with its native promoter was cloned into the binary vector pCubi1390. The construct was then introduced into the *fse6* callus by an Agrobacterium-mediated transformation method (Zhu et al. 2018). Basic Local Alignment Search Tool (BLAST) analysis in the National Center for Biotechnology Information (NCBI, <http://www.ncbi.nlm.nih.gov>) was used to identify *FSE6* homologues among different species. A phylogenetic tree of neighbor-joining was constructed by MAGA 5.0 (<http://www.megasoftware.net>). The amino acid sequences were aligned using DNAMAN 6.0 (<https://www.lynnon.com/dnmana.n.html>), and secondary structure of the encoded protein was predicted using Jalview 2.11. (<http://www.jalview.org/>).

β-Glucuronidase (GUS) Staining

The 2 kb nucleotide sequence upstream of *OsFSE6* ATG was introduced into the pCAMBIA1381Z vector and then the construct was transformed into NG4. The positive plants were identified by PCR and used for GUS staining as described previously (Zheng et al. 2015).

Subcellular Localization of OsFSE6

The full-length coding sequence of *OsFSE6* was cloned into the pCAMBIA1305 vector with a green fluorescent protein (GFP) tag to produce 1305-*OsFSE6*-GFP construct. Then the construct was transformed into EHA105 Agrobacterium and infected leaf epidermal cells of *Nicotiana benthamiana*. GmMan1 and VSR2 were used as markers of Golgi and pre-vacuolar compartments (PVCs), respectively. GFP alone was used as the control and fluorescent images were observed by a Leica confocal laser scanning microscope (SP8, Leica).

RNA Extraction and Real-Time PCR

Total RNA was isolated from specific tissues including roots, stems, leaves, sheaths, panicles and developing endosperms at 6–21 DAF using an RNAPrep Pure Plant Kit (Tiangen Biotech, Beijing). RNA concentrations were measured using Nanodrop 2000 (Thermo Scientific, USA). About

2 μg total RNA was immediately reverse-transcribed with oligo(dT)₁₈ primer following the manufacturer's instructions of the PrimeScript Reverse Transcriptase kit (TaKaRa, Tokyo). Primers used in real-time fluorescence PCR were shown in Table S1.

Protein Extraction and Immunoblot Analysis

About 20 mg mature seeds or endosperm sample was ground into powder in a 2 mL tube and 400 μL protein extraction solution [12.5% (v/v) 1 M Tris-HCl (pH 6.8), 5% β-mercaptoethanol (v/v), 4% sodium dodecyl sulfate (SDS) and 24% Urea (w/v) and suitable Bromophenol blue] was added. Then the sample was mixed well by vortexing and kept overnight in 50°C. The supernatant was centrifuged at 12,000 g and collected for SDS polyacrylamide gel electrophoresis (SDS-PAGE). After that, the protein was transferred to a polyvinylidene fluoride (PVDF) membrane at 100 mA. Protein immunoblotting with corresponding antibodies was detected with electrochemiluminescence (ECL) reagent (Bio-Rad).

Determination of Cellulose Content and Hydrogen Peroxide Content

Seedlings of NG4 and *fse6* were dried at 50 °C and ground into powder and filtered through 80 mesh sieves. In a boiling water bath, the sample was treated with an acetic acid/nitric acid reagent (H₂O: CH₃COOH:HNO₃ = 90:360:45) for at least 30 min. The supernatant was discarded after centrifugation at 13,000g. The above steps were repeated three times and the precipitate was washed once with distilled water. The precipitate was dissolved with 72% concentrated sulfuric acid overnight. The sample and the 0.2% anthrone solution were kept in a boiling water bath for reaction. Based on the absorbance of 620 nm, the cellulose content of the sample was calculated.

To determine the content of hydrogen peroxide, 0.5 g rice leaves were firstly cut into pieces and grind into 2 mL homogenate with pH 7.4 phosphate buffered saline (PBS). After centrifugation at 9000 g for 15 min, the supernatant was taken for measurement using a hydrogen peroxide assay kit (<http://www.njcbio.com/>).

Acknowledgements This research was supported by Key Laboratory of Biology, Genetics and Breeding of Japonica Rice in Mid-lower Yangtze River, Ministry of Agriculture, P. R. China, Jiangsu Collaborative Innovation Center for Modern Crop Production. This research was supported by the National Transformation Science and Technology Program (2016ZX08001006), the National Key Research and Development Program of China (2016YFD0100500), Jiangsu Science and Technology Development Program (BE2018388), and Jiangsu Province Agriculture Independent Innovation Fund Project (SCX(19)1079). This work was also supported by the Fundamental Research Funds for the

Central Universities (KYTZ201601) and the Postgraduate Research & Practice Innovation Program of Jiangsu Province (KYCX20_0578).

Author Contributions HY and LLL performed phenotypic analysis, gene mapping, gene cloning, data analysis and wrote the manuscript; KW performed phenotype analysis and gene mapping; JL, SJL, XL and YLT determined the physical and chemical properties of rice grains; RBC and XLC measured the cellulose and hydrogen peroxide content of rice seedlings; YLW, ECD and XHB performed the subcellular localization and western blot analysis; YJ and YZ performed RT-qPCR; YHW and LLL revised the manuscript; JMW and YHW designed the experiments and revised the manuscript. All the authors agreed on the contents of the paper and post no conflicting interest.

References

- Baldwin TC, Handford MG, Yuseff M-I, Orellana A, Dupree P (2001) Identification and characterization of GONST1, a golgi-localized GDP-mannose transporter in Arabidopsis. *Plant Cell* 13(10):2283–2295
- Burrell MM (2003) Starch: the need for improved quality or quantity—an overview. *J Exp Bot* 54(382):451–456
- Chen M, Han G, Dietrich CR, Dunn TM, Cahoon EB (2007) The essential nature of sphingolipids in plants as revealed by the functional identification and characterization of the Arabidopsis LCB1 subunit of serine palmitoyltransferase[W]. *Plant Cell* 18(12):3576–3593
- Dunn TM, Lynch DV, Michaelson LV, Napier JA (2004) A post-genomic approach to understanding sphingolipid metabolism in *Arabidopsis thaliana*. *Ann Bot* 5:483–497
- Ekstrom A, Taujale R, McGinn N, Yin Y (2014) PlantCAZyme: a database for plant carbohydrate-active enzymes. *Database (Oxford)* 2014:1–8
- Fang L, Ishikawa T, Rennie EA, Murawska GM, Lao J, Yan J, Tsai AY, Baidoo EEK, Xu J, Keasling JD (2016) Loss of inositol phosphorylceramide sphingolipid mannosylation induces plant immune responses and reduces cellulose content in Arabidopsis. *Plant Cell* 28:2991–3004
- Hao Y, Wang Y, Wu M, Zhu X, Teng X, Sun Y, Zhu J, Zhang Y, Jing R, Lei J, Li J, Bao X, Wang C, Wang Y, Wan J (2019) The nuclear-localized PPR protein OsNPPR1 is important for mitochondrial function and endosperm development in rice. *J Exp Bot* 70(18):4705–4720
- Ishikawa T, Fang L, Rennie EA, Sechet J, Yan JW, Jing BB, Moore W, Cahoon EB, Scheller HV, Kawai-Yamada M, Mortimer JC (2018) GLUCOSAMINE INOSITOLPHOSPHORYLCERAMIDE TRANSFERASE1 (GINT1) Is a GlcNAc-containing glycosylinositol phosphorylceramide glycosyltransferase. *Plant Physiol* 177(3):938–952
- Jean-Luc C, Corinne B, Kevin G, Patricia G-P, Jeannine L (2016) Revisiting plant plasma membrane lipids in tobacco: a focus on sphingolipids. *Plant Physiol* 170:367–384
- Kang HG, Park S, Matsuoka M, An G (2005) White-core endosperm flour endosperm-4 in rice is generated by knockout mutations in the C4-type pyruvate orthophosphate dikinase gene (OsPPDKB). *Plant J* 42(6):901–911
- Liu L, Ma X, Liu S, Zhu C, Ling J, Wang Y, Yi S, Ren Y, Hui D, Chen L (2009) Identification and characterization of a novel Waxyl allele from a Yunnan rice landrace. *Plant Mol Biol* 71(6):609–626
- Markham JE, Jaworski JG (2007) Rapid measurement of sphingolipids from *Arabidopsis thaliana* by reversed-phase high-performance liquid chromatography coupled to electrospray ionization tandem mass spectrometry. *Rapid Commun Mass Spectrom* 21(7):1304–1314
- McFarlane HE, Doring A, Persson S (2014) The cell biology of cellulose synthesis. *Annu Rev Plant Biol* 65:69–94
- Miao Y, Yan PK, Kim H, Hwang I, Jianga AL (2006) Localization of GFP fusions with the seven Arabidopsis vacuolar sorting receptors to prevacuolar compartments in tobacco BY-2 cells. *Plant Physiol* 142:945–962
- Mongrand S, Morel J, Laroche J, Claverol S, Carde JP, Hartmann MA, Bonneu M, Simon-Plas F, Lessire R, Bessoule JJ (2004) Lipid rafts in higher plant cells: purification and characterization of triton X-100-insoluble microdomains from tobacco plasma membrane. *J Biol Chem* 279(35):36277–36286
- Mortimer JC, Yu X, Albrecht S, Sicilia F, Huichalaf M, Ampuero D, Michaelson LV, Murphy AM, Matsunaga T, Kurz S, Stephens E, Baldwin TC, Ishii T, Napier JA, Weber AP, Handford MG, Dupree P (2013) Abnormal glycosphingolipid mannosylation triggers salicylic acid-mediated responses in Arabidopsis. *Plant Cell* 25(5):1881–1894
- Peng C, Wang Y, Liu F, Ren Y, Zhou K, Lv J, Zheng M, Zhao S, Zhang L, Wang C (2014) FLOURY ENDOSPERM6 encodes a CBM48 domain-containing protein involved in compound granule formation and starch synthesis in rice endosperm. *Plant J* 77(6):917–930
- Perotto S, Donovan N, Drobak BK, Brewin NJ (1995) Differential expression of a glycosyl inositol phospholipid antigen on the peribacteroid membrane during pea nodule development. *Mol Plant Microbe Interact* 8(4):560–568
- Rennie EA, Ebert B, Miles GP, Cahoon RE, Christiansen KM, Stonebloom S, Khatab H, Twell D, Petzold CJ, Adams PD (2014) Identification of a sphingolipid α -glucuronosyltransferase that is essential for pollen function in Arabidopsis. *Plant Cell* 26(8):3314–3325
- Seung D, Smith AM (2019) Starch granule initiation and morphogenesis—progress in Arabidopsis and cereals. *J Exp Bot* 70(3):771–784
- Singh SK, Eland C, Harholt J, Scheller HV, Marchant A (2005) Cell adhesion in *Arabidopsis thaliana* is mediated by ECTOPICALLY PARTING CELLS 1—a glycosyltransferase (GT64) related to the animal exostosins. *Plant J* 43:384–397
- Takemoto Y, Coughlan SJ, Okita TW, Satoh H, Ogawa M, Kumamaru T (2002) The rice mutant esp2 greatly accumulates the glutenin precursor and deletes the protein disulfide isomerase. *Plant Physiol* 128(4):1212–1222
- Tartaglio V, Rennie EA, Cahoon R, Wang G, Scheller HV (2016) Glycosylation of inositol phosphorylceramide sphingolipids is required for normal growth and reproduction in Arabidopsis. *Plant J Cell Mol Biol* 89(2):278–290
- Wang W, Yang X, Tangchaiburana S, Ndeh R, Markham JE, Tsegaye Y, Dunn TM, Wang G-L, Bellizzi M, Parsons JF (2008) An inositolphosphorylceramide synthase is involved in regulation of plant programmed cell death associated with defense in Arabidopsis. *Plant Cell* 20(11):3163–3179
- Wu M, Ren Y, Cai M, Wang Y, Zhu S, Zhu J, Hao Y, Teng X, Zhu X, Jing R, Zhang H, Zhong M, Wang Y, Lei C, Zhang X, Guo X, Cheng Z, Lin Q, Wang J, Jiang L, Bao Y, Wang Y, Wan J (2019) Rice FLOURY ENDOSPERM10 encodes a pentatricopeptide repeat protein that is essential for the trans-splicing of mitochondrial nad1 intron 1 and endosperm development. *New Phytol* 223(2):736–750
- You X, Zhang W, Hu J, Jing R, Cai Y, Feng Z, Kong F, Zhang J, Yan H, Chen W, Chen X, Ma J, Tang X, Wang P, Zhu S, Liu L, Jiang L, Wan J (2019) FLOURY ENDOSPERM15 encodes a glyoxalase I involved in compound granule formation and starch synthesis in rice endosperm. *Plant Cell Rep* 38(3):345–359
- Zhang L, Ren Y, Lu B, Yang C, Feng Z, Liu Z, Chen J, Ma W, Wang Y, Yu X, Wang Y, Zhang W, Wang Y, Liu S, Wu F, Zhang X,

- Guo X, Bao Y, Jiang L, Wan J (2016) FLOURY ENDOSPERM7 encodes a regulator of starch synthesis and amyloplast development essential for peripheral endosperm development in rice. *J Exp Bot* 67(3):633–647
- Zheng M, Yihua W, Yunlong W, Chunming W, Yulong W, Jia L, Cheng P, Tao W (2015) DEFORMED FLORAL ORGAN1 (DFO1) regulates floral organ identity by epigenetically repressing the expression of OsMADS58 in rice (*Oryza sativa*). *New Phytol* 206(4):14
- Zhu X, Teng X, Wang Y, Hao Y, Jing R, Wang Y, Liu Y, Zhu J, Wu M, Zhong M (2018) FLOURY ENDOSPERM11 encoding a plastid heat shock protein 70 is essential for amyloplast development in rice. *Plant Sci* 277:89–99